Electronic Supplementary Material (ESI) for Physical Chemistry Chemical Physics.

Hyaluronan biopolymers release water upon pH-induced gelation

Eliane P. van Dam, Giulia Giubertoni, Federica Burla, Gijsje H. Koenderink and Huib J. Bakker*[a]

Supplementary Information

S1. Experimental methods – Pump Probe Spectroscopy

We prepare hyaluronic acid solutions by dissolving 20 mg high- or low-molecular weight hyaluronan (hyaluronic acid sodium salt from *Streptococcus equi*, ~1.5-1.8 MDa, Sigma Aldrich, or sodium hyaluronate, Research grade, 100-150 kDa, Lifecore Biomedical, respectively) in 1 ml solution containing 150 mM sodium chloride (NaCl, 99.5%, Sigma Aldrich) and 4% D_2O (99.9%D, Cambridge Isotope laboratories) in H_2O (ultrapure milli-Q grade). We adjust the pH by adding an amount of perchloric acid ($HClO_4$, standard solution 1M, Fluka Sigma Aldrich). Perchloric acid was used, because this acid has only a very small contribution to the water signal in the anisotropy experiments. This is due to the fact that the OD groups of HDO molecules hydrogen bonded to the perchlorate anion (ClO_4^-) absorb at a significantly higher frequency (~2650 cm^{-1}) than the OD groups forming hydrogen bonds to the oxygen atoms of water molecules or hyaluronan (~2500 cm^{-1}). The samples were mixed using a vortex mixer and left to equilibrate for at least 12 hours, and used for a maximum time of one week, since the samples can eventually undergo hydrolytic degradation.

We performed femtosecond mid-infrared transient absorption measurements on solutions of high and low molecular weight hyaluronic acid, in the pH range from pH 1.5 to pH 4.2. To this end, we pump and probe the OD stretch vibrations of HDO molecules with 200 femtosecond pulses centered at 2500 cm^{-1}. These pump and probe pulses are created by frequency conversion of the output of a Yb:KGW (ytterbium doped potassium gadolinium tungstate) based laser system (Pharos, Light Conversion) using a tunable OPA (Orpheus-ONE-HP, Light Conversion). The laser produces 400 µJ pulses, with a wavelength of 1028 nm and a repetition rate of 50 kHz. Using a pulse picker we reduce the repetition rate to 1 kHz. In a first frequency conversion step, white light that was generated using part of the laser light is parametrically amplified in two BBO crystals. These optical parametric amplification (OPA) processes are pumped with the second harmonic of the laser light (515 nm). The OPA processes result in intense light pulses that are tunable from 680 to 850 nm and from 1350 to 2060 nm. The latter pulse is used as an input seed pulse in a third OPA process in a KTA crystal that is pumped with the residual fraction of the fundamental of the pump laser. This OPA process results in a strong signal pulse (1350-2060 nm) and an idler (2060-4500 nm) pulse. With this method we generated idler pulses at 4000 nm (2500 cm^{-1}) that we used in a pump-probe experiment. These pulses have an energy of 12 µJ, a bandwidth of 100 cm^{-1}, and a pulse duration of 200 fs. The probe pulse is created by splitting off a small part of the pulses with a ZnSe beamsplitter. The transmitted probe pulses were detected using a spectrometer in combination with a 3 x 32 pixel MCT detector.

The pump pulse excites part of the OD stretch vibrations, and the resulting absorption changes are probed using the probe pulse. We measure the change in absorption as a function of the time delay between the pump and probe. The probe pulse is polarized either parallel or perpendicular to the polarization direction

[a] E.P. van Dam, G. Giubertoni, F. Burla, Prof. Dr. G.H. Koenderink, Prof. Dr. H.J.Bakker
AMOLF
Science Park 104, 1098 XG Amsterdam (The Netherlands)

of the pump pulse. Directly after pump excitation, the measured absorption change will be larger in the parallel direction ($^{\Delta\alpha}{}_{\parallel}$(v,t)) than in the perpendicular direction ($^{\Delta\alpha}{}_{\perp}$(v,t)), because the pump excites the vibrations that are oriented parallel to the polarization of the pump pulse most efficiently. When the delay time between pump and probe is increased, the difference between the two signals decreases due to the reorientation of the HDO molecules. From the parallel and perpendicular signals we construct the reorientation independent isotropic signal:

$$\Delta\alpha_{iso}(v,t) = \frac{1}{3}(\Delta\alpha_{\parallel}(v,t) + 2\Delta\alpha_{\perp}(v,t))$$

The isotropic signal decays with the vibrational lifetime. At longer time delays we observe a thermal difference spectrum. We subtract this ingrowing heating signal by fitting the transient spectra to a kinetic model that describes the relaxation of the excited OD stretch vibrations via an intermediate state to a thermalized hot ground state. After correcting the measured absorption changes $^{\Delta\alpha}{}_{\parallel}$(v,t) and $^{\Delta\alpha}{}_{\perp}$(v,t) for the ingrowing heating signal, we construct the vibrational relaxation independent anisotropy R:

$$R(v,t) = \frac{\Delta\alpha_{\parallel}(v,t) - \Delta\alpha_{\perp}(v,t)}{\Delta\alpha_{\parallel}(v,t) + 2\Delta\alpha_{\perp}(v,t)}$$

The dynamics of the anisotropy represent the reorientation dynamics of the water hydroxyl groups present in the solution.[1]

Pump-probe data analysis

A brief summary of the data analysis is described here. A more detailed description can be found in references[1–3]. The isotropic spectra, as shown in Figure 1A, show a negative signal at early time delays at the frequency of the OD stretch vibration. This negative signal is indicative of the ground-state bleach. At long time delays, we observe a long-living spectral signature with the shape of the thermal difference spectrum. This thermal difference spectrum is due to the heating of the sample after excitation and the following relaxation of the OD oscillators. To extract our anisotropic signal associated with the excitation of the OD oscillators, without the influence of the heating, we subtract the ingrowing heating contribution. We do this by fitting the spectra to a kinetic model that describes the vibrational relaxation of the excitation of the OD stretch vibration via an intermediate state to the heated ground state. In this model, the intermediate state accounts for the delayed rise of the heating and has no transient spectrum. Before calculating the anisotropy, the spectral component associated with the heating effect was subtracted from $^{\Delta\alpha}{}_{\parallel}$ and $^{\Delta\alpha}{}_{\perp}$, assuming the heated ground state to be isotropic. The anisotropy is then calculated using the formula above.

S2. Experimental methods - Rheology

Sample preparation for the rheology measurement

The samples were prepared in a glass vial by first weighing and adding hyaluronic acid sodium salt in powder form (Streptococcus equii, Sigma Aldrich, 1.5-1.8 MDa molecular weight), and subsequently adding water, NaCl (Sigma Aldrich), and HCl (Sigma Aldrich) to achieve different molarities of HCl (ranging from 0-60 mM), 0.15 M NaCl and a final concentration of 10 mg/mL hyaluronic acid. The samples were left to equilibrate at room temperature until they were homogeneous. After equilibration, for each sample the pH was measured using a pH meter (Hanna Instruments). The pH values as a function of concentration of acid can be found in S3.

Rheology measurements

The rheological properties of the solutions were measured with a stress-controlled rheometer (Anton Paar Physics MCR 501) using a PP40 geometry (parallel plates, 40 mm diameter) at a 100 µm gap and at a temperature of 22°C set by a Peltier system. The elastic and viscous shear moduli were probed by oscillatory shear rheology, with an oscillation frequency of 0.5 Hz and a small strain amplitude of 0.5% to ensure a linear response. At each pH we averaged the results of at least three measurements.

DDM experiments

Differential dynamic microscopy (DDM) measurements were done using probe particles with diameters of 0.6 µm, from Sigma Aldrich (Latex beads, polystyrene). In order to avoid non-specific interactions of the particles with hyaluronan, the particles were passivated with poly(ethylene glycol) chains following an established protocol.[5] The beads were added to the hyaluronan gels in a ratio of 1:100 (v/v) and the samples were vortexed to ensure a homogeneous distribution of the particles. The samples were then placed between two coverslips (Menzel™ Microscope Coverslips 24x60mm, #1, Thermo Scientific) separated by a silicone chamber (Grace Bio-Labs CultureWell™ chambered coverglass, Sigma Aldrich). The samples were imaged in bright field mode on an inverted Ti-Eclipse microscope (Nikon) with a 100x oil immersion objective and a fast camera (Hamamatsu, Orca-Flash 4.0). The samples were imaged at least 10 um above the surface to avoid non-specific interactions with the glass slides. Videos of 5000 frames were recorded with a frame rate of 100 frames per second and an exposure time of 10 ms. The measurement was repeated in at least three different portions of the sample.

DDM analysis

The videos obtained were analysed with a custom written MatLab program. The principle of the techniques were introduced in Ref.[6] The thermal motion of the particles in the viscous medium causes fluctuations of the intensity. The recorded intensity I (x,y,t) is transformed to the Fourier space and the images measured at different lag times Δt can be correlated to obtain the image structure function:

$$D\,(q,\Delta t) = < |i(q,t+\Delta t) - i(q,t)|^2 > ,$$

where q is the wavevector, which is defined as $q=2\pi/\lambda$

Next, the intermediate scattering function can be obtained from the image structure function through the formula:

$$D\,(q,\Delta t) = A(q)[1 - f(q,\Delta t)] + B(q)$$

Here A(q) is a proportionality factor between the intensity and the correlation fluctuations, while B(q) represents the noise of the camera.

By fitting the intermediate scattering function f(q,Δt) to a stretched exponential decay $e^{-(\frac{\Delta t}{\tau(q)})^n}$, it is possible to retrieve the diffusion coefficient of the particle $D = 1/(\tau(q)q^2)$. In all of the cases examined, the fit yielded a value of n=1, indicating simple diffusion.

We infer the viscosity η of the solution from the generalized Stokes-Einstein relation:

$$D_m = \frac{k_B T}{6\pi\eta a}$$

Where a is the particle radius. The viscosities were obtained from correlation functions recorded at a q-value of 7.2 µm^(-1) units, and the values shown are an average over data obtained from three different locations in the sample.

S3. pH measurements of low molecular weight hyaluronic acid

$[HClO_4]$ (mmolal)	pH
0	6.91±0.03
3	4.16±0.04
8	3.67±0.02
13	3.39±0.12
22	3.06±0.10
31	2.75±0.07
38	2.57±0.00
44	2.43±0.09
45	2.38±0.11
51	2.24±0.11
54	2.05±0.07
60	1.88±0.08
70	1.71±0.07
83	1.51±0.05

Table S1. Measured pH values at different $HClO_4$ concentrations for 20 mg/ml low molecular weight hyaluronic acid.

S4. $HClO_4$ measurements

The measured hyaluronic acid solutions were prepared in 150 mM NaCl. We adjusted the pH value of the solution by adding perchloric acid ($HClO_4$). Next to hyaluronic acid, the other components (Na^+, Cl^- H^+ and ClO_4^-) present in the solution can contribute to the offset R_{slow} in the anisotropy decay. In order to examine the magnitude of this contribution and to correct for this, we measured the anisotropy of the excited OD stretch vibration of HDO molecules in solutions of 150 mM NaCl and different concentrations of $HClO_4^-$ in isotopically diluted water. Figure 1 shows the anisotropy decay as a function of delay time for similar $HClO_4$ concentrations that were used in the measurements of the solutions containing hyaluronic acid. We observe that the anisotropy of the different solutions is very similar to that of neat isotopically diluted water. When we look closely at the later delay times, from 4 to 7 picoseconds, as in Figure 1B, we see that with increasing $HClO_4^-$ concentration, there is a small, yet significant, increasing offset.

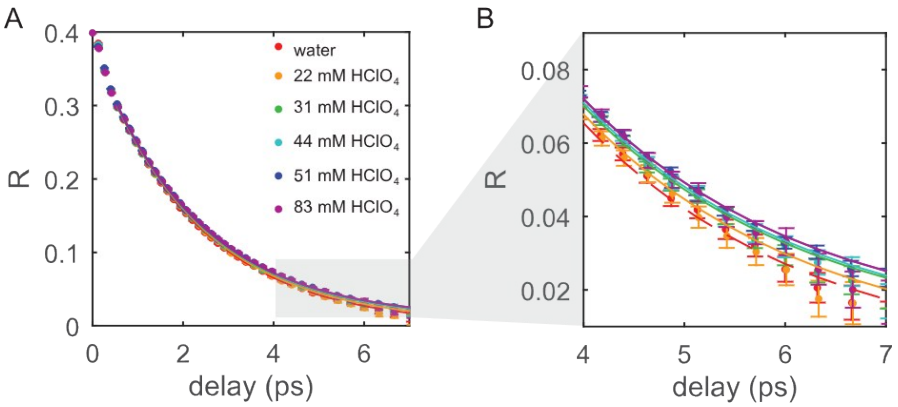

Figure S1. (A) Anisotropy decay as function of delay time for different solutions of $HClO_4$ in 150 mM NaCl in isotopically diluted water and neat isotopically diluted water, The solid lines are fits to an exponential function with an offset. (B) Detail of the anisotropy decay.

The normalized offsets are depicted in Figure 2 as a function of the $HClO_4$ concentration. The blue points represent the offset of solutions only containing $HClO_4$. The offset clearly increases with increasing $HClO_4$ concentration. For a solution without $HClO_4$, the offset is not zero because all solutions contain 150 mM NaCl, contributing to the offset. The data points were fitted with a linear function y=ax+b. From the slope of this function we conclude that 10±3 OH groups per ClO_4^- ion are slowed down, and from the offset it follows that 9±1 OH groups are slowed down by an Na^+ ion plus a Cl^- ion.

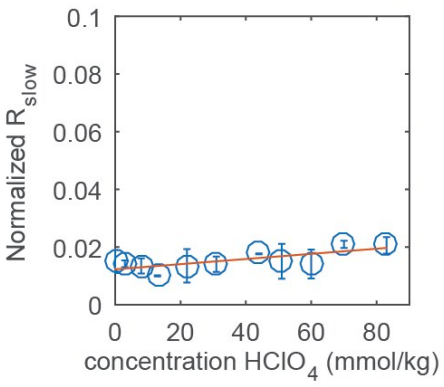

Figure S2. Offset of the anisotropy decay as a function of $HClO_4$ concentration for solutions only containing $HClO_4$. All solutions are in isotopically diluted water and also contain 150 mM NaCl. The solid line is a guide to the eye.

S5. Values of R_0, R_{slow} and $R_{slow}/(R_{slow}+R_0)$

High Molecular Weight

$[HClO_4]$ (mmolal)	R_0	R_{slow}	$R_{slow}/(R_{slow}+R_0)$
3	0.3701±0.0014	0.0179±0.0005	0.0461±0.0013
8	0.3817±0.0003	0.0169±0.0010	0.0425±0.0023
13	0.3664±0.0019	0.0164±0.0005	0.0428±0.0010
22	0.3746±0.0010	0.0149±0.0004	0.0382±0.0009
31	0.3714±0.0004	0.0154±0.0002	0.0399±0.0005
44	0.3818±0.0015	0.0085±0.0001	0.0218±0.0001
45	0.3719±0.000004	0.0111±0.0019	0.0290±0.0049
51	0.3810±0.0024	0.0121±0.0012	0.0306±0.0029
54	0.3712±0.0039	0.0164±0.0010	0.0422±0.0029
60	0.3700±0.0009	0.0209±0.0008	0.0536±0.0021
70	0.3787±0.0016	0.0150±0.0018	0.0380±0.0043
83	0.3783±0.0012	0.0127±0.0006	0.0324±0.0016

Low molecular weight

$[HClO_4]$ (mmolal)	R_0	R_{slow}	$R_{slow}/(R_{slow}+R_0)$
3	0.3735±0.0008	0.0158±0.0005	0.0405±0.0013
8	0.3751±0.0008	0.0147±0.0002	0.0377±0.0006
13	0.3697±0.0008	0.0140±0.0008	0.0365±0.0021
22	0.3755±0.0022	0.0152±0.0032	0.0389±0.0081
31	0.3721±0.0021	0.0143±0.0013	0.0369±0.0032
38	0.3718±0.0063	0.0155±0.0016	0.0402±0.0045
44	0.3720±0.0010	0.0166±0.0009	0.0427±0.0022
45	0.3703±0.0011	0.0142±0.0012	0.0369±0.0029
51	0.3725±0.0020	0.0120±0.0007	0.0312±0.0017
54	0.3744±0.0022	0.0109±0.0003	0.0282±0.0008
60	0.3736±0.0003	0.0178±0.0020	0.0453±0.0049
70	0.3719±0.0013	0.0171±0.0026	0.0440±0.0066
83	0.3767±0.0012	0.0159±0.0020	0.0406±0.0050

$HClO_4$

$[HClO_4]$ (mmolal)	R_0	R_{slow}	$R_{slow}/(R_{slow}+R_0)$
0	0.3747±0.0004	0.0057±0.0015	0.015±0.0040
3	0.3726±0.0011	0.0054±0.0005	0.0142±0.0012
8	0.3744±0.0032	0.0050±0.0010	0.0135±0.0026
13	0.3757±0.0007	0.0038±0.0001	0.0100±0.0002
22	0.3759±0.0018	0.0051±0.0022	0.0135±0.0058
31	0.3739±0.0028	0.0053±0.0010	0.0140±0.0026

44	0.3721±0.0014	0.0067±0.0001	0.0177±0.0002
51	0.3763±0.0014	0.0057±0.0023	0.0151±0.0060
60	0.3748±0.0014	0.0054±0.0019	0.0141±0.0050
70	0.3717±0.0021	0.0079±0.0005	0.0209±0.0012
83	0.3701±0.007	0.0078±0.0011	0.0206±0.0029

Table S2. Values of R_0, R_{slow} and $R_{slow}/(R_{slow}+R_0)$ at different $HClO_4$ concentrations for the high molecular weight, low molecular weight and $HClO_4$ measurements series. The $R_{slow}/(R_{slow}+R_0)$ values are shown figure 3 and figure 5 in the main text.

S6. pKa determination low-molecular weight hyaluronic acid

Fit of the linear infrared absorption spectra at different $HClO_4$ concentrations.

Linear infrared spectroscopy was used to determine the pK_a of hyaluronic acid by measuring the spectra in the frequency region of the absorption bands of the carboxylate anion and carboxylic acid groups as a function of pH. The amplitudes of the bands are indeed directly proportional to the concentration of –*COOH* and -*COO*$^-$ present in the solution. In the deprotonated state, the anti-symmetric stretching mode of the carboxylate anion group is absorbing at 1607 cm^{-1}, whilst in the protonated state the carbonyl stretching of the –*COOH* absorbs at 1725 cm^{-1}. Unfortunately, this kind of titration measurements to determine the pK_a can be done only by using heavy water solvent so to avoid the overlap with the strong bending absorption band of the water at 1643 cm^{-1}. In order to determine the pK_a in water we study the absorption band of the symmetric stretching vibration of the –COO$^-$, which absorbs around 1410 cm^{-1}. The cross-section of this vibration is smaller than the one of the anti-symmetric stretching mode, but somewhat larger than the one of the –CH modes absorbing in the same frequency region (Fig.S3a).[7] We can so clearly observe the vibration at 1412 cm^{-1}. We observe that the band decreases in intensity by lowering pH. At strongly acidic pH we observe a residual absorption due to the presence of a broad –CH band centered around 1420 cm^{-1}. Furthermore, we observe that there is a strong contribution of the background due to the presence of HDO bending vibration at 1450 cm^{-1}.

We thus fit the linear infrared spectra using a global fitting procedure as a function of frequency and pH (which we directly measure by using a glass-electrode), which is based on the minimization of the square error

$$\sum_{i,j}\left(S(\omega_j,pH_i) - S^{exp}(\omega_j,pH_i)\right)^2 \qquad (1)$$

where **S** is the fitted spectrum and $\mathbf{S^{exp}}$ the experimental spectrum. We assume that the experimental spectra are a linear combination of the spectra at neutral, $\mathbf{S_n}$, and acidic (pH=1.5), $\mathbf{S_a}$, pH. To compensate for the effect of the background we also add the water spectrum $\mathbf{S_w}$. We thus expect that

$$\forall i, for\ \omega_{\{min\}} \leq \omega_J \leq \omega_{\{max\}}$$
$$S(\omega_j, pH_i) = c_n S_n(\omega_j, pH_i)^{neutral} + c_a S_a(\omega_j, pH_i)^{acid} + c_w S_w(\omega_j, pH_i) \qquad (2)$$

where c_n,c_a and c_w are the coefficient for the neutral, acid and background spectra, respectively. The c_n and c_a represent the fraction of neutral hyaluronic acid $[HA]^{ext}$ and deprotonated hyaluronic acid $[A^-]^{ext}$ at different pH.

Calculation of the pK_a value in water.

By measuring directly the pH of the solutions and extracting the concentration of the protonated and deprotonated species, we can determine the pK_a using the acid-base equilibrium and mass balance equations:

$$con_{hyal.acid} = [HA] + [A^-]$$

(3)

$$pK_a = pH - \log_{10}\frac{[A^-]}{[HA]}$$

(4)

The first equation represents the conservation of the analytical concentration $con_{hyal.acid}$ of hyaluronic acid, that at every pH has to be preserved as the sum of neutral hyaluronic acid $[HA]$ and negatively charged hyaluronic acid $[A^-]$. The second equation represents the acid-base equilibrium equation for hyaluronic acid. In order to extract the pK_a, we fit the fractions of $[HA]^{ext}$ and $[A^-]^{ext}$ (extracted from the global fit of the linear spectra), by using a global fitting procedure as a function of pH. This procedure is based on the minimization of the least-square error of the following expression:

$$\sum_i ([HA]^{ext}(pH_i) - \frac{[HA]}{con_{hyal.acid}}(pH_i, pK_a))^2 + \sum_i ([A^-]^{ext}(pH_i) - \frac{[A^-]}{con_{hyal.acid}}(pH_i, pK_a))^2$$

(5)

where pK_a is the only free parameter. We obtain from the fit a value of $pK_a = 2.9 \pm 0.2$ that is in good agreement with the value found for high molecular weight hyaluronic acid.[4]

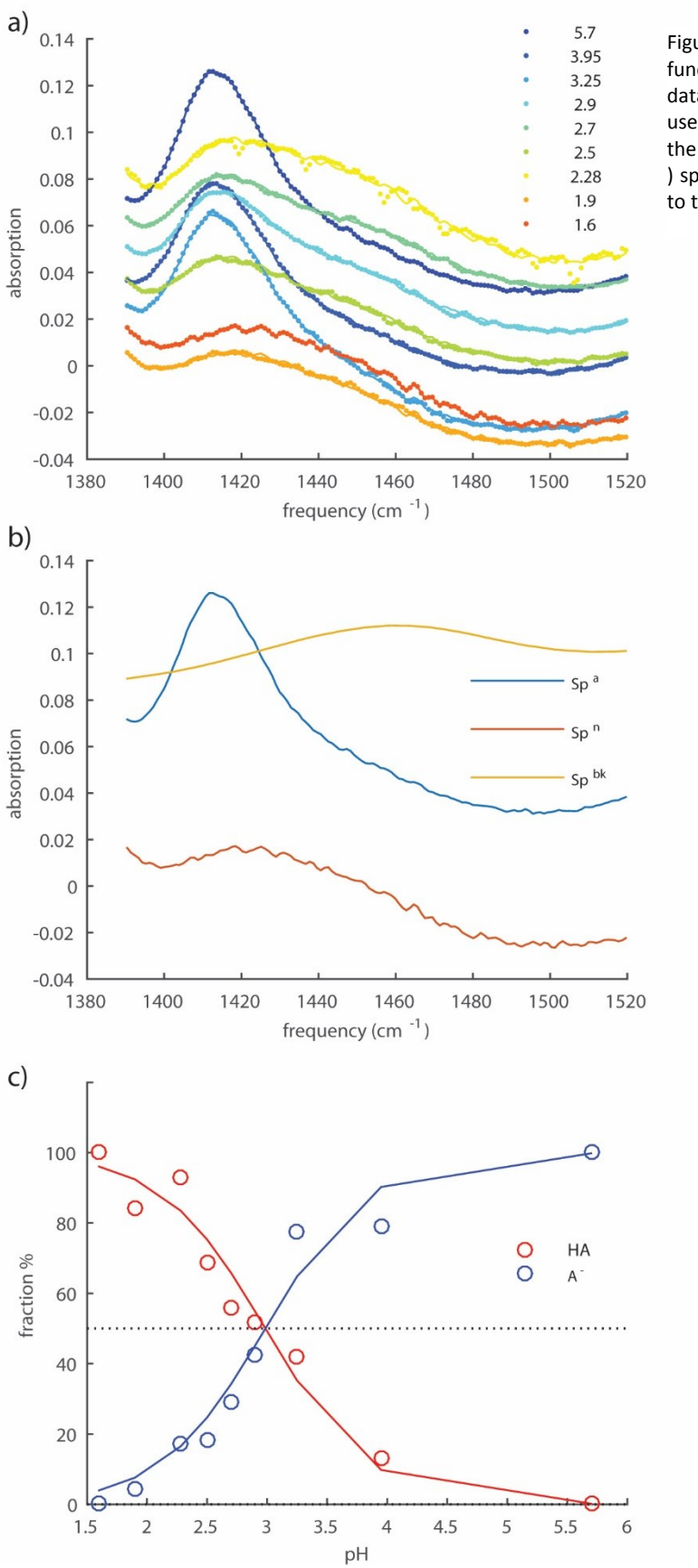

Figure S3: a) Fit and experimental linear spectra as a function of pH. Dotted lines represent experimental data, continuous line fit data. b) Spectral signatures used to fit the data in a). c) Circles points represent the fraction of protonated (*HA*) and deprotonated (A^-) species as a function of pH. Continuous line are fit to the model described in eq.(3) and (4).

References

1 Y. L. A. Rezus and H. J. Bakker, *J. Chem. Phys.*, , DOI:10.1063/1.2009729.

2 T. Steinel, J. B. Asbury, J. Zheng and M. D. Fayer, *J. Phys. Chem. A*, 2004, **108**, 10957–10964.

3 Y. L. A. Rezus and H. J. Bakker, *Phys. Rev. Lett.*, 2007, **99**, 1–4.

4 G. Giubertoni, F. Burla, C. Martinez-Torres, B. Dutta, G. Pletikapic, E. Pelan, Y. L. A. Rezus, G. H. Koenderink and H. J. Bakker, *J. Phys. Chem. B*, 2019, **123**, 3043–3049.

5 A. J. Kim, V. N. Manoharan and J. C. Crocker, *J. Am. Chem. Soc.*, 2005, **127**, 1592–1593.

6 R. Cerbino and V. Trappe, *Phys. Rev. Lett.*, 2008, **100**, 1–4.

7 A. Kovács, B. Nyerges and V. Izvekov, *J. Phys. Chem. B*, 2008, **112**, 5728–35.